



## Microstructure and crystallography in Axophyllinae. Precisions on the genus *Morenaphyllum*

Ismael CORONADO<sup>1,2\*</sup> & Sergio RODRÍGUEZ<sup>1,3</sup>

<sup>1</sup> Departamento de Paleontología, Universidad Complutense de Madrid. c/ José Antonio Nováis 12, Ciudad Universitaria. E-28040 Madrid. Spain; ismael.coronado@geo.ucm.es

<sup>2</sup> Institute of Paleobiology, Twarda 51/55, PL-00-818 Warsaw (Poland)

<sup>3</sup> Instituto de Geociencias (IGEO. CSIC-UCM). c/ José Antonio Nováis 12, Ciudad Universitaria. E-28040 Madrid. Spain

\* Corresponding author

Coronado, I. & Rodríguez, S. 2018. Microstructure and crystallography in Axophyllinae. Precisions on the genus *Morenaphyllum*. [Microestructura y cristalografía en Axophyllinae. Precisiones sobre el género *Morenaphyllum*]. *Spanish Journal of Palaeontology*, 33 (1), 41-56.

---

Manuscript received 10 December 2016

Manuscript accepted 7 December 2017

© Sociedad Española de Paleontología ISSN 2255-0550

---

### ABSTRACT

The microstructure of the genus *Morenaphyllum* has been studied in ultrathin sections by means of petrographic microscopy and computer integrated polarization microscopy (CIP). Although the studied specimens are partially recrystallized, the microstructure can be observed in zones that are quite well preserved. *Morenaphyllum* shows walls composed of lamellae piled in bundles, lamellar dissepiments, tabulae and stereoplastic thickenings and septa composed of small fibres that change their orientation from the periphery to the axial zones of the coral. In spite of the presence of some peculiarities, this microstructure fit well with that described in other Axophyllinae.

**Keywords:** Biocrystallization, Paleozoic corals, crystallographic orientation, CIP.

### RESUMEN

La microestructura del género *Morenaphyllum* se ha estudiado mediante secciones ultrafinas con microscopio petrográfico y con microscopía de polarización integrada por ordenador (CIP). Aunque los ejemplares estudiados presentan cierto nivel de recristalización, la microestructura se reconoce en muchas zonas aceptablemente preservadas. *Morenaphyllum* presenta murallas constituidas por fascículos de lamelas apiladas, disepimentos, tábulae y estereoplasma lamelar y septos formados por fibrillas que cambian su orientación desde las zonas periféricas del coral a las más axiales. Dicha microestructura concuerda en general con lo observado en los Axophyllinae, aunque muestra algunas variaciones con respecto a otros géneros de la familia.

**Palabras clave:** Biocrystalización, corales paleozoicos, orientación cristalográfica, CIP.

## 1. INTRODUCTION

Axophyllinae are solitary rugose corals showing axial structure and transeptal (lonsdaleoid) dissepiments that have been recently revised by Rodríguez & Somerville (2015). The Axophyllinae are common in the upper Mississippian and lowermost Pennsylvanian from Palaeotethys and they are important in biostratigraphic, palaeogeographic and paleoecologic studies (Rodríguez & Somerville, 2015 and references herein). The microstructure of Axophyllinae is quite consistent and homogeneous in all genera of the family (Rodríguez & Somerville, 2015). Most of Axophyllinae show granulo-fibrous or fibrous septa (mesoplasm) and lamellar wall, tabulae, dissepiments and thickenings of septa (stereoplasm). However, there are some variations that will be described in this paper based on the analysis of several specimens (the holotype included) of *Morenaphyllum antolinense* Rodríguez & Somerville, 2015.

Their macrostructures are well known, but most authors that revised this subfamily did not describe their microstructure (Gorsky, 1938, 1951; Sayutina, 1973; Poty, 1981). Other authors described it only superficially (Rodríguez, 1984; Gómez-Herguedas & Rodríguez, 2005; Rodríguez & Said, 2010; Rodríguez & Somerville, 2015). Only Semenoff-Tian-Chansky (1974) analysed in depth the microstructure of several genera. The study of the microstructure of Axophyllinae is important, because they show consistently lamellar microstructure in many of their skeletal elements in all studied outcrops and stratigraphic units. But lamellar microstructure is controversial because it has been regarded by many authors as result of diagenesis (Kato, 1963; Sorauf, 1971, 1978, 1983; Oekentorp, 1984, 2001). On the contrary, other authors have regarded it as primary and used it as taxonomical criteria both, in tabulate and rugose corals (Lafuste, 1978, 1981, 1983; Lafuste & Plusquellec, 1985; Rodríguez, 1984, 1989, 2004; Falces, 1997; Rodríguez & Somerville, 2015). Recent studies on tabulate corals using techniques of mineral characterization at different scales (including crystallographic and geochemical methods) demonstrated without doubt that lamellar microstructures are primary in Tabulates (Coronado *et al.*, 2013, 2015a, 2015b, 2015c; Coronado & Rodríguez, 2016) and in Devonian Rugosans (Coronado *et al.*, 2016). These studies have highlighted the biogenic origin of the microstructures of Paleozoic corals, shedding light on crystallization processes, the assembly mechanisms and summarizing the abiogenic crystallochemical characteristics specific to diagenetic alteration of these microstructures. Diagenesis is common in Paleozoic fossils and should be identified to advance in the knowledge of evolutionary biocrystallization processes.

The main subject of this paper is the detailed microstructural description of the Axophyllinae and more

precisely of the genus *Morenaphyllum* Rodríguez & Somerville, 2015 and its comparison with other Paleozoic corals previously described.

## 2. GEOLOGICAL SETTING

The Guadiato Area (Fig. 1) has been usually included in the Ossa-Morena Zone, which is divided in structural domains defined by Chacón *et al.* (1974) and Delgado-Quesada *et al.* (1977). The Carboniferous rocks from Guadiato Valley were divided in three bands (Southern, Central and Northern) by Pérez-Lorente (1979). Our studies allowed the identification of three tectonostratigraphic units in the central and southern bands (Cózar & Rodríguez, 1999): Fresnedoso Unit, Sierra del Castillo Unit and San Antonio-La Juliana Unit. The Sierra del Castillo, in which our study is focused, is composed of several blocks containing mainly upper Viséan marine carbonate rocks.

The Antolín outcrops are located in the northwestern margin of the Sierra Boyera Block (Fig. 1). It comprises the Boyera ridge and several hills at northwest. It is composed of turbiditic sandstones and shales, with common interbedded limestone debris (Cózar & Rodríguez, 2000; Rodríguez & Rodríguez-Curt, 2002). The coral assemblage from Antolín (Rodríguez *et al.*, 2016) occurs in limestone breccias containing reefal, shallow platform and upper talus slope facies (Rodríguez & Rodríguez-Curt, 2002). Three sections (Antolín 1, 2 and 3) have been measured in that area (Fig. 1). The studied corals have been recorded in the lower beds of Antolín 2 section.

The limestone breccias from Antolín show a chaotic distribution. They show much carbonatic matrix between the clasts that are heterometric, from millimetres to more than 1 meter in diameter. There are also many bioclasts, mainly crinoids, brachiopods and corals. It was interpreted as a proximal turbidite (Rodríguez & Rodríguez-Curt, 2002).

## 3. MATERIAL AND METHODS

The studied specimens are the holotypes, paratypes and topotypes of *Morenaphyllum antolinense* that have been recorded in the Brigantian from Antolín outcrop, Sierra Morena, SW Spain (see Rodríguez & Somerville, 2015). The methods used in the study of the microstructures of a genus of Axophyllinae have been petrographic microscopy and computer integrated polarization microscopy (CIP) (Coronado *et al.*, 2015a). Nineteen ultrathin sections of transverse and longitudinal sections of several ontogenic stages of *Morenaphyllum antolinense* were used for these methods. The method of preparation of ultrathin sections to

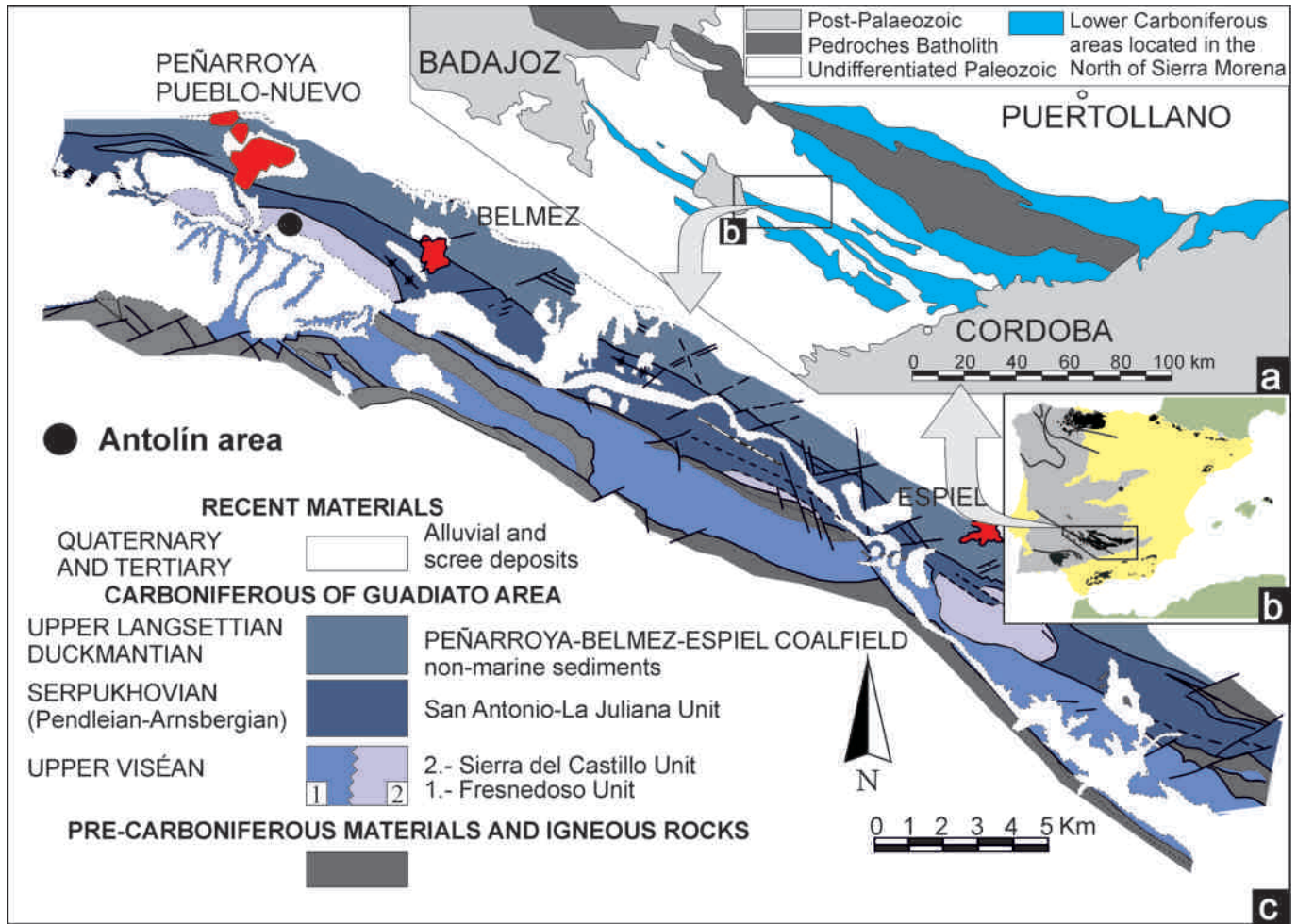


**Figure 1. a)** Early Carboniferous outcrops (upper Tournaisian to Arnsbergian) in the northern Sierra Morena. **b)** Synthetic map showing the distribution of the main Carboniferous outcrops of the Iberian Peninsula (black pattern). Modified from Colmenero *et al.* (2002). **c)** Synthetic map of the main geological units of the Guadiato Area. Modified from Cózar & Rodríguez (1999).

study the microstructure was developed by Lafuste (1970). For the analysis of thin sections by CIP it is necessary to use ultra-thin sections due to the size of crystals, when the first-second order of interference colour is reached (grey to blue colorations). In the case of Paleozoic corals this colouration is reached when the thin section is between 2 and 10  $\mu\text{m}$  in thickness (Coronado *et al.*, 2015a), due to the thickness of calcite crystals.

The samples were systematically microphotographed and the microcrystals have been measured by the micrographs using the plugin ObjectJ 1.03w (Vischer *et al.*, 1994) of ImageJ 1.47v (Abramoff *et al.*, 2004) free and open image processing software.

The CIP method (computer-integrated-polarization microscopy) has been described by Heilbronner & Pauli (1993), Heilbronner (2000), and Heilbronner & Barret (2014) as a method for texture analysis and optical orientation imaging and used in structural geology studies. It determines the *c*-axis orientations of uniaxial minerals (as calcite and quartz) from optical micrographs,

displaying the results in the form of pole figures and orientation images, using a colour-code (CLUT), which represents each orientation. This method has been applied to biomineralization studies of fossil Paleozoic corals with relevant results (Coronado *et al.*, 2015a, 2015c; Coronado & Rodríguez, 2016; Coronado *et al.*, 2016), allowing obtaining quickly crystallographic, structural and diagenetic information. One advantage of this technique applied to biomineralization studies is the quick processing of data at different scales, working easily at 4x to 40x magnifications (at mesoscale to microscale), covering large areas and with low cost.

Seven CIP analyses in different samples and structural elements (wall, dissepiments, septa and their variations) were performed using an experimental petrographic Zeiss microscope with an automated rotation and tilting system, confectioned with the Arduino UNO microcontroller (open-source hardware) and controlled with software was implemented in LabVIEW environment, for first time employed in this article. The microscope has a reflex

camera Canon EOS 70D attached and an interference filter ELP of 645 nm favouring the colour separation and the micrographs processing for CIP method. The analysis have been performed at 6.3x, 10x and 20x magnifications (resolution of 5472 x 3648 pixel and the lower ratio pixel- $\mu\text{m}$  reached is 1:0.1, 1:0.05 at 40x). The micrographs were processed with the Image SXM software (Barret, 1997) to determine the crystallographic arrangement of coral skeleton microstructure.

Crystallographic techniques have been applied in numerous contributions as robust tools for detection of alteration by diagenesis in fossils (Coronado *et al.*, 2015a, 2015b; Cummings *et al.*, 2014; Grellet-Tinner *et al.*, 2011; Pérez-Huerta *et al.*, 2007). The controlled biominerals that compose the skeletons of Paleozoic corals lose the preferential crystallography orientation during the diagenesis (Cummings *et al.*, 2014; Coronado *et al.*, 2013, 2015b). The processes of dissolution - coprecipitation can be slow and kept the morphological features of crystals, but the original crystallographic orientation is lost. On this basis, misorientation images were analysed to characterise the potential diagenetical alteration of these coral samples (Coronado *et al.*, 2015a for details). These images show the misorientation, which is the number of degrees required

to bring these two points into crystallographic alignment on a common axis (Dalbeck *et al.*, 2006), for each pixel measured in north-south direction and their variation in inclination. Microstructural descriptions are based on the terminology proposed by Semenov-Tian-Chansky (1974) with some refinements by Rodríguez (1984).

## 4. RESULTS

### 4.1 Macroscopic features of *Morenaphyllum*

The genus *Morenaphyllum* is an Axophyllinae and consequently it comprises solitary corals with variable axial structure comprising median lamella joined to the cardinal septum and septal lamellae and having lonsdaleoid dissepiments. The diagnostic features of the genus that distinguish it from other genera of the subfamily are a small axial structure joined to a thick and long cardinal septum; a conspicuous inner wall composed of lamellar thickenings and a wide transeptal dissepimentarium (Fig. 2).

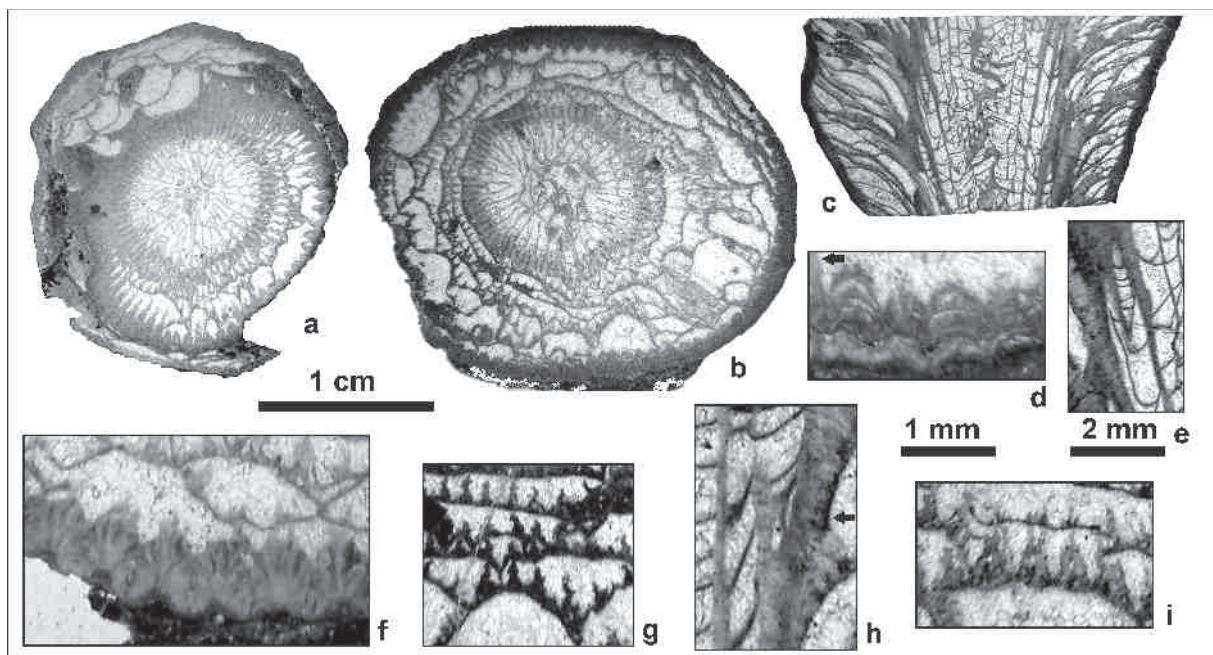


**Figure 2.** *Morenaphyllum antolinense* Rodríguez & Somerville, 2015. **(a-f)** Specimen ANT2/2-52 (holotype), **(a)** transverse section in early adult stage. **(b)** Transverse section in advanced adult stage. **(c)** Longitudinal section. **(d)** Detail showing naotic septa (black arrow) and lamellar fascicles in the wall and on the dissepiments **(e)** detail showing biform tabularium in longitudinal section. **(f)** Detail showing lamellar fascicles in the wall. **(g)** Specimen ANT2/2-44 (paratype), detail of the spines on the lonsdaleoid dissepiments and fibrous septa cut in longitudinal section. **(h)** Specimen ANT2/2-33 (paratype), detail of biform tabularium and fibers in the septa cut in longitudinal section (black arrow). **(i)** Specimen ANT2/2-14 (paratype), detail showing spines on the lonsdaleoid dissepiments. Figures (a-c), scale bar = 1 cm. Figures (d, f-i), scale bar = 1 mm. Figure (e), scale bar = 2 mm.

## 4.2. Microstructural characterization

*Morenaphyllum antolinense* skeletons have a variable microstructure along of different structural elements. Two conspicuous microstructural elements have been identified: lamellae and fibres, with different developments and morphologies. A detailed description of each structural element in all areas of the coral is performed with the purpose of characterizing the microstructure.

### 4.2.1. Thick wall

A thick wall with an undulated or festooned internal outline is characteristic of this taxon at mesoscale (Fig. 3a). The microstructure is mainly lamellar (*sensu* Lafuste, 1983), composed of curved or slightly undulated crystals (lamellae, >25  $\mu\text{m}$  *sensu* Rodríguez, 1989), with indentation at their edges and lengths from 29 to 49  $\mu\text{m}$  (mean = 32  $\mu\text{m}$ ) and width from 4 to 9  $\mu\text{m}$  (mean = 7  $\mu\text{m}$ ). The development in width gives an appearance of “cupular” lamellae, whereas the undulated are “scutellate” (Fig. 3b). Lamellae at the wall are completely imbricated showing a compact frame, which at mesoscale looks like undulated with festoon-like structures in contact each other. At microscale the festoon-like structures are formed by piles or rows of lamellae disposed in fascicles (as can be distinguished by the interference colour); at the contact surface between two festoons the crystals are truncated and the interference colour change abruptly (Fig. 3b). In the undulated outline of festoon-like structures between two lamellae rows the lamellae gradually change to fibres forming tepee-like structures (Fig. 3b). The fibres are short and irregular. It is usual to observe primary cements growing in contact with the fibres, which have the same interference coloration.

### 4.2.2. Septa

Septa are growing in continuity with the wall, and in juvenile stages the septa are thick and form a thick peripheral stereozone (Fig. 3c). It is common to observe the septa growing on lonsdaleoid dissepiments in transversal section of adult stages, giving the appearance of discontinuous septa (Fig. 2b). At microscale the septa have a blurred homogeneous microstructure formed by small pseudo-grains of 3-5  $\mu\text{m}$  of diameter, but oblique sections show septa composed of elongated fibres (Figs. 3d-e). Small irregular fibres with indented edges are the most common microstructure in septa, with lengths from 19 to 44  $\mu\text{m}$  (mean = 30  $\mu\text{m}$ ) and width from 3 to 6 (mean = 4  $\mu\text{m}$ ). In transverse sections, it is observed that the long and straight septa have a median line formed by the pseudo-granular looks-like, which is derived from perpendicular sectioning of fibres. Laterally the fibres grew straight and regular with a palisade looks-like (Fig. 3f). The axial part

of the septa shows a fasciculate appearance in the tip with curved fibres growing to each side (Fig. 3f).

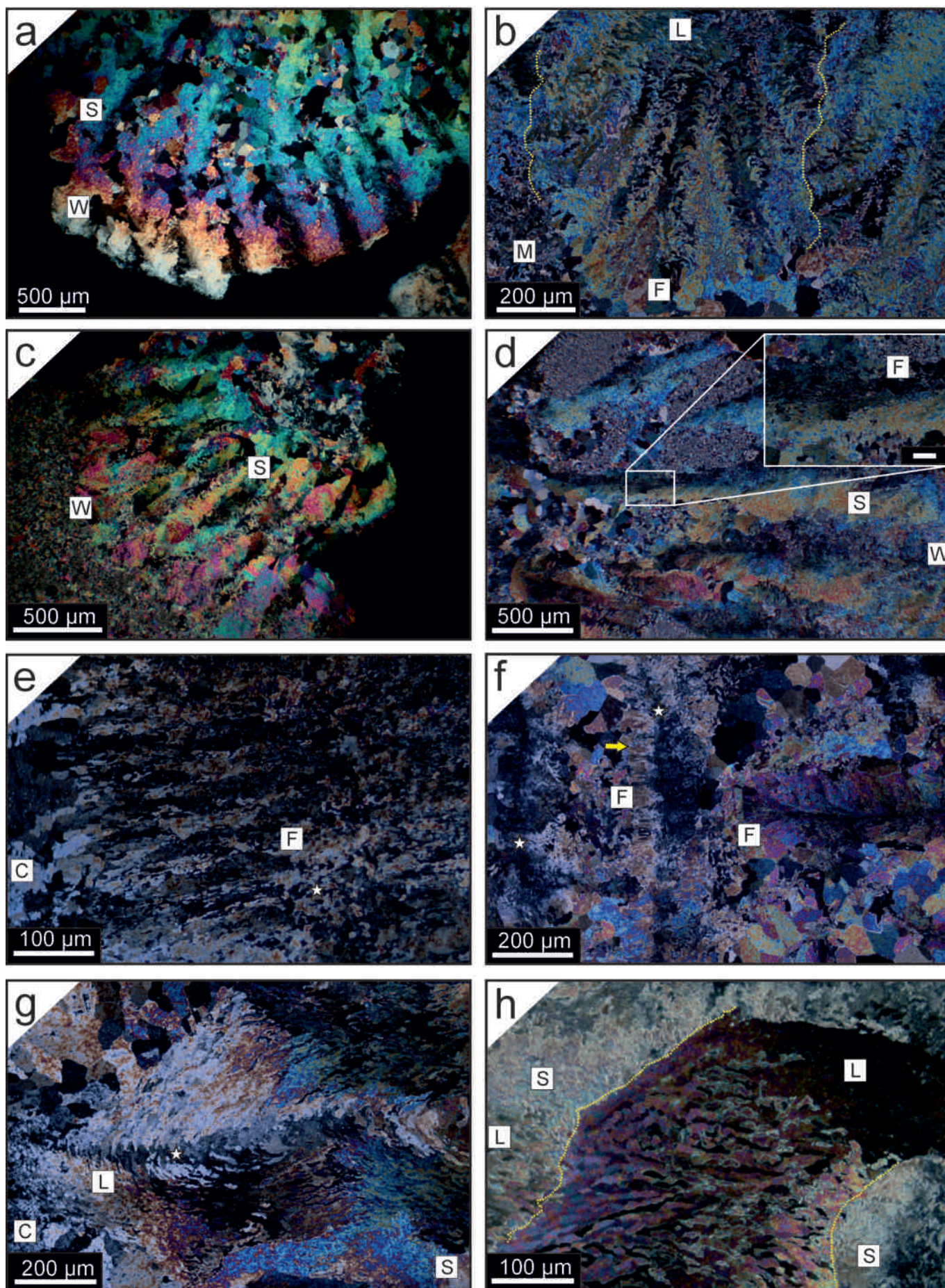
Stereoplasm thickenings in the inner wall and between septa are composed of lamellae, stacked and completely imbricated. Lamellae are thick “scutellate” at straight areas or with curved morphologies at narrowing areas, adapting to the shape of stereoplasm (Fig. 3g). The lamellar crystals are strongly undulated (Fig. 3h), with curve indentations in their edges and lengths from 18 to 90  $\mu\text{m}$  (mean = 43  $\mu\text{m}$ ) and width from 4 to 13  $\mu\text{m}$  (mean = 8  $\mu\text{m}$ ). The stereoplasm thickening is deposited between structures such as septa and the wall and on the dissepiments and tabulae. In those deposits the lamellae are curved adapting their morphological axis to the microstructure of the septa (Fig. 3h).

### 4.2.3. Axial structure

The axial structure of *Morenaphyllum* is an irregular median plate composed by the thicker cardinal septum, radial lamellae and axial tabellae (Figs 4a-b). The microstructure is difficult to recognize due to the amalgamation and disarray of structural elements. The lamellae are filling and thickening the median plate, with curved and irregular crystals. Fibres are also present, and grew from septa interdigitating in the structure and covering the external area of median plate and septa. All the elements are complexly imbricated (Fig. 4b), with gradual morphological transitions between different crystal domains (from lamellae of thickening deposits to fibres). The size of crystal units is very variable, from microlamellae in the pass of septum fringe to large lamellae in the thickening deposits. Microlamella with lengths from 11 to 36  $\mu\text{m}$  (mean = 19  $\mu\text{m}$ ) and width from 2 to 9 (mean = 4  $\mu\text{m}$ ), looks like flakes in some sections and lamellae show lengths from 20 to 63  $\mu\text{m}$  (mean = 43  $\mu\text{m}$ ) and widths from 5 to 17 (mean = 9  $\mu\text{m}$ ). The fibres have the same dimension as in the septa.

### 4.2.4. Tabulae and dissepiments

Tabulae and dissepiments are composed of lamellae, although some dissepiments have also small fibre fascicles at both sides (Fig. 4c). When the thickening of dissepiment continues, in transeptal dissepiments, they form crests at mesoscale, with a characteristic denticulations (Fig. 4d). The lamellae are forming piles or small fasciculate rows and the ending are topped by sort irregular fibres forming a spiky structure. The lamellae are mainly “scutellate” in dissepiments, although plier-shape is common in the transeptal dissepiments (Fig. 4d). The crystals have a lateral development in two dimensions, with lengths from 13 to 74  $\mu\text{m}$  (mean = 38  $\mu\text{m}$ ) and width from 4 to 15  $\mu\text{m}$  (mean = 8  $\mu\text{m}$ ).



### 4.3. Crystallographic characterization

Computer-integrated-polarization microscopy (CIP) has been used with the purpose of identify the crystallographic arrangement and preservation state of microstructure at mesoscale and microscale in different structural parts of skeleton. Six c-axis orientation images (COI) in transverse and longitudinal section and their corresponding pole-figures were obtained using the CIP method from different elements: two in the wall area, one in a transeptal dissepiment, one in a contact between stereoplasm thickenings and a septa and two in septa. The crystallographic arrangement will be explained in terms of azimuth and inclination of c-axis, being the azimuth the orientation in regard of referenced system marked by micrograph position.

All the COI show common crystallographic features with the c-axis oriented perpendicular to morphological axis in lamellae and parallel to fibres. Therefore the c-axis is always oriented toward the axial edge of coral. In those occasions where the microstructural elements rotate, as occur in the stereoplasm thickenings in the inner wall, the c-axis rotate with them, as can be denoted by interference colour of Figure 3g. The transverse sections of corals exhibit a common pole maxima ca. 20-30° of inclination toward the axial edge.

The thick wall formed by festoon-like structures has a radiate crystallographic arrangement with two different crystallographic domains easily distinguished (Figs 5a-d): a fasciculate looks-like with lamellar rows and an inner area with a stacking of lamellae. That inner area, depending of sectioning, can be a lamellar sclerenchima growing laterally, with inclinations ca. 60° (Figs 5a-b) or almost perpendicular to surface of wall (Figs 5c-d). The pole figure of Figure 5b has a small pole maximum more vertical than the Figure 5d. The wall sectioned in Figures 5a-b (point 1 in Fig. 5I) has difference in inclination of ca. 40° of inner area (point 2 in Fig. 5I) according to the rows of lamellae. On regard to azimuthal dispersion the rows are separated ca. 40° among them (Fig. 5II). The truncation of lamellae between different festoon-like structures in contact and the fasciculate distribution of rows of lamellae suggest

a competitive growth from a base line, similarly observed in other Paleozoic corals (Coronado *et al.*, 2015b, 2016).

Some areas of wall are altered by diagenesis (Figs 5a, 5c, 7). The contact area of wall and the matrix have some indications of recrystallization: as degrading neomorphism and random crystallographic orientations. The misorientation images (Coronado *et al.*, 2015a) of north-south and inclination (details in Heilbronner & Barret, 2014) verify these observations (Fig. 7). The contact areas have a marked different crystallographic alignment of c-axis in terms of azimuth and inclination.

Dissepiments were analysed in an area in contact of two transeptal dissepiments. They are composed of fasciculate rows of lamellae. The right lateral of micrograph shows a continuous growth of these rows along two dissepiments (Fig. 5f), keeping the crystallographic orientation. Unlike with the thick wall, the azimuthal distribution between rows is less dispersed, ca. 10° (Fig. 5III), although the inclination is ca. 30°, as occur in the thick wall, because both growth forming fascicles. The c-axis orientation is similar between fibres and lamellae and despite of the gradual transition between morphologies the crystallographic orientation is kept.

A COI of stereoplasm in contact with a septum has been got to asset the relation between different structures. The COI and pole figure suggest that the septal fibres (S in Figs 6a-b) have a strong inclination, ca. 60° whereas laterally the fibres turn ca. 30° of inclination. In the contact with the septa the lamellae of stereoplasm have the same crystallographic orientation and inclination. The lamellae of stereoplasm have a very narrow distribution as can be seen by isolines of pole maxima, suggesting a great crystallographic control of the sclerenchima overgrowth.

The misorientation images show diagenetic alteration in the limit of stereoplasm and the inner cement, characterized by random crystallographic orientations (Figs 6I, 7). It should be highlighted that at the left side of the micrograph the morphology of lamellae is preserved despite of recrystallization. Syntaxial cement includes these altered crystals keeping their morphological aspect.

**Figure 3.** Microscopic features of *Morenaphyllum*. C: cement; F: fibres; L: lamellae; M: matrix; S: septum; W: wall. **a)** Specimen IC-01. Transverse section showing the festoon-like structures and their relation with septa at mesoscale. **b)** Specimen IC-04. Detail of festoon-like area in the contact point of three fascicles (dotted yellow lines). **c)** Specimen IC-05. Micrograph of a transverse section of a juvenile specimen showing the thick peripheral stereozone. **d)** Specimen IC-13. Transverse section showing the microstructure of straight septa. Inset of septum, showing the fibrous microstructure. **e)** Specimen IC-06. Longitudinal section showing the irregular and short fibres of septa. **f)** Specimen IC-18. Transverse section of a young coral showing an axial septa with a fasciculate tip (yellow arrow) and a long septa with pseudo-granular appearance of the middle lamina of septa (white stars) and the palisade looks-like of external fringe (yellow arrow). **g)** Specimen IC-12. Longitudinal section of an adult stage showing the lamellar stereoplasm rotating. Note the undulating lamellae and the domical in the narrow zones (white star). **h)** Specimen IC-13. Transverse section showing a lamellar stereoplasm growing between two septa. Yellow dotted lines mark the contact area.

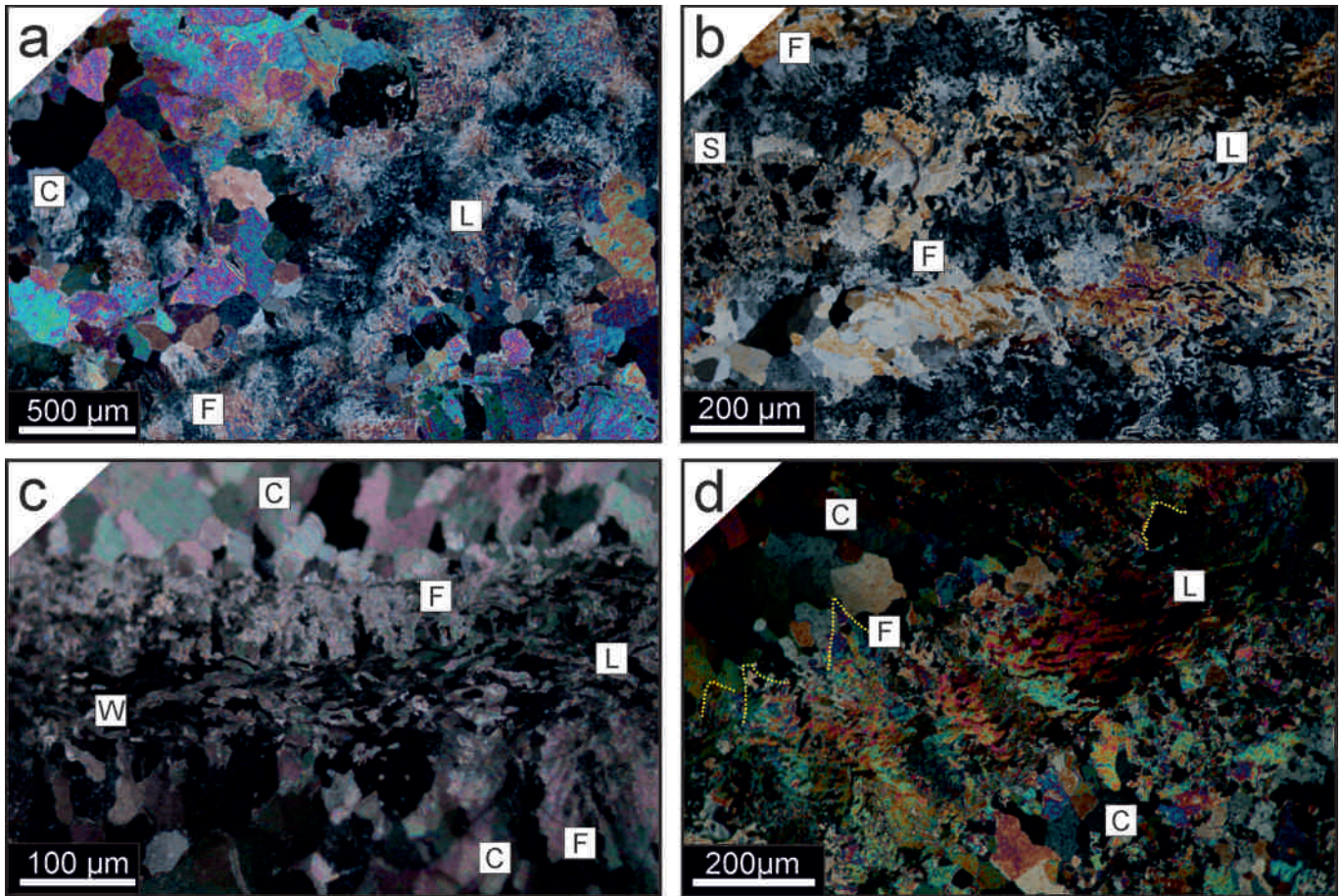


**Figure 4.** Microscopic features of *Morenaphyllum*. C: cement; F: fibres; L: lamellae;  $\mu$ L: microlamellae; S: septum; W: wall. **a-b)** Specimen IC-14. Transverse section showing an axial structure of *Morenaphyllum*. **(a)** The contact area between cardinal septa, radial lamellae and axial tabellae. **(b)** Detail of microstructure, showing the complex structuration and the transition between fibres and lamellae through microlamellae. **c-d)** Specimen IC-12. Longitudinal section showing the microstructure of a dissepiment. **(c)** Note the fascicles of fibres to both sides. **(d)** Note the plier-shape in this transeptal dissepiments and the spiky structure formed by fibres in the fringe.

The septa have been studied in two different zones, in the contact with the wall (Figs 6c-d) and in an area with short septa and the stereoplasm thickenings (Figs 6e-f). Those are composed by lamellae of different sizes and morphologies and fibres. The c-axis orientation in septa is very narrow, being sharper in the sort septa in relation with the long septa. Figures 6c-d show a gradual transition between the wall and the septa. The long septa have an azimuthal distribution of ca.  $10^\circ$ , whereas the wall has an azimuthal distribution of ca.  $40^\circ$ . This distribution has been identified in other Paleozoic corals as part of circular distribution of sclerenchyma. The inclination along the insertion of septa and the wall changes gradually ca.  $30^\circ$  (points 1 and 2 in Fig. 6II). On the contrary, the short septa are composed of fibres and the stereoplasm thickening is composed of large lamellae and transitional microlamellae. The azimuthal distribution of this micrograph is separate in three main directions, one for each structure. The lamellar stereoplasm have a low inclination in regard of septa ca.  $30^\circ$

(points 1 and 2 in Fig. 6III). The COI show the marked azimuthal distribution between the structures (Fig. 6e).

Figure 7 represents the misorientation images of three COI selected, in north-south and inclination analysis. As can be observed, the altered areas in the external fringes of skeletons (Fig. 7) exhibit random crystallographic orientations, with strong changes in the misorientation images (abrupt coloration changes).

## 5. DISCUSSION

The microstructure of axophyllid corals has been only systematically described by Semenoff-Tian-Chansky (1974) and Rodríguez & Somerville (2015). The diagnosis and descriptions of the different genera are very consistent in the microstructure. In all cases, the wall, tabulae,

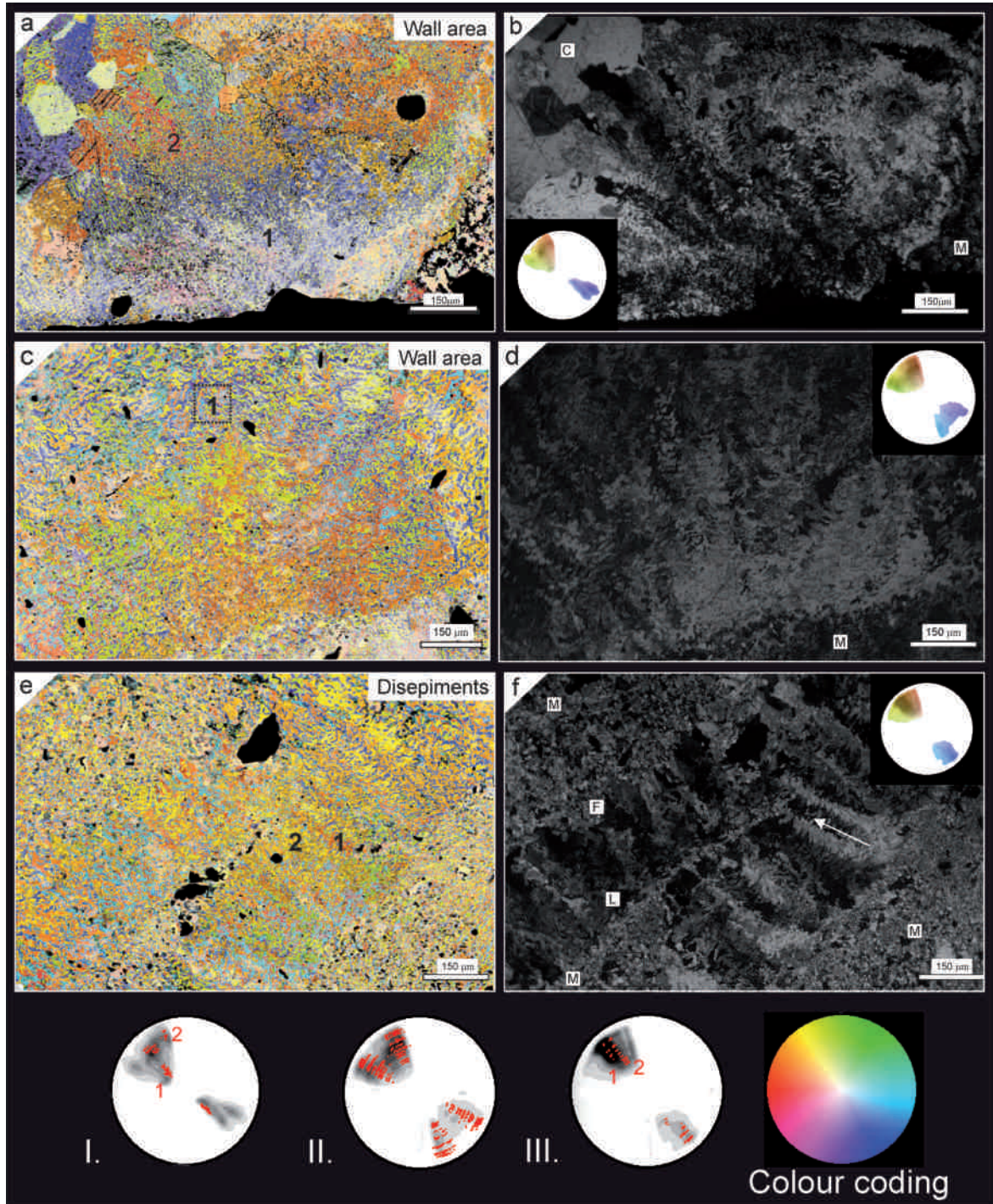
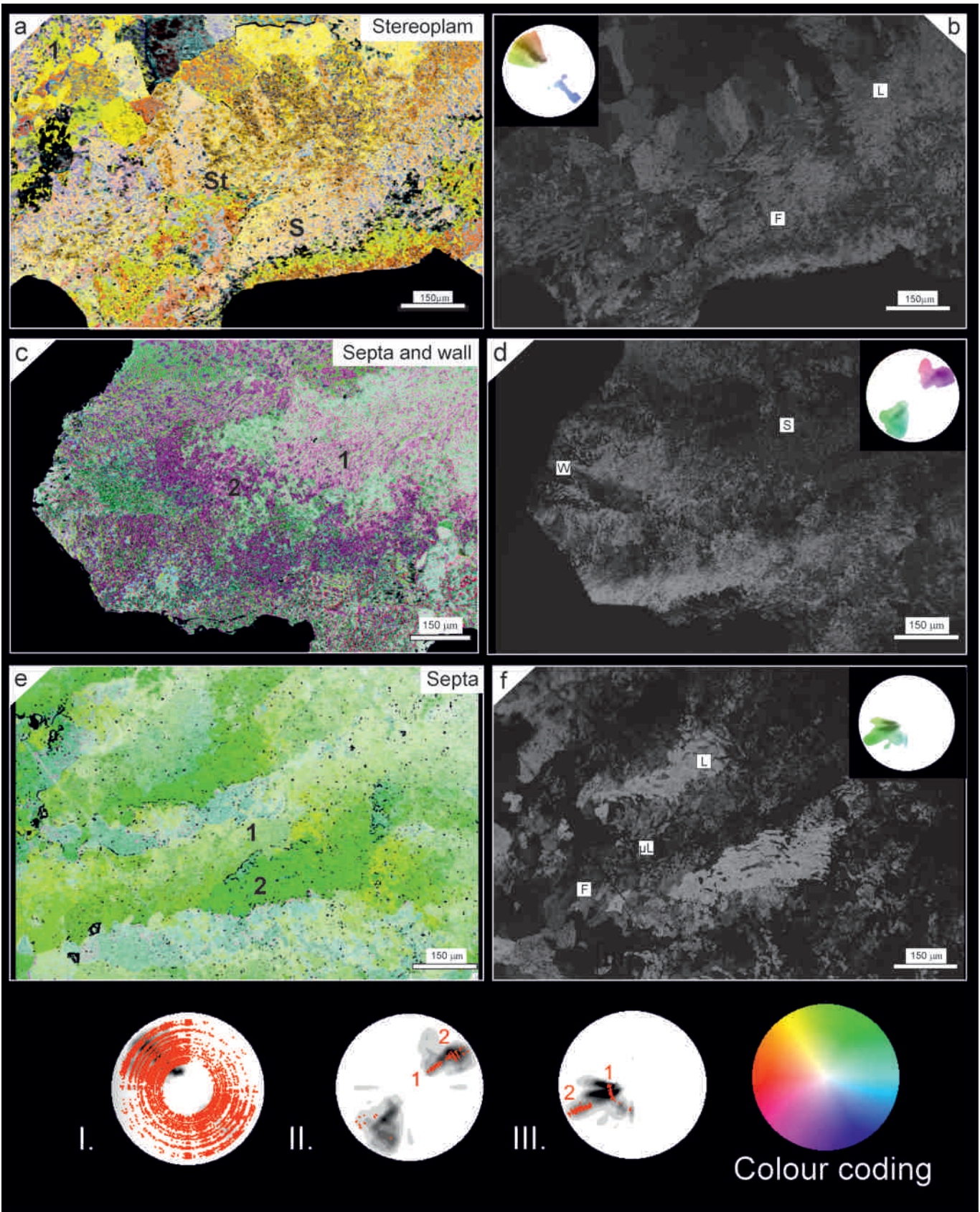


**Figure 5.** CIP analysis of a transverse (a-c) and longitudinal (e-f) sections of *Morenaphyllum*. C: cement; F: fibres; M: matrix; L: lamellae. **a)** Specimen IC-01. Orientation image of a wall area. Points 1 and 2 correspond with selected regions plotted in (I) **b)** Petrographic micrograph of the wall area showing the fasciculate arrangement of lamellae. Inset showing the pole figure of the entire investigated area. **c)** Specimen IC-14. Orientation image of the wall area showing the fasciculate arrangement of lamellae. Point 1 corresponds with the selected region plotted in (II) **d)** Petrographic micrograph of the studied area (scale bar = 150  $\mu\text{m}$ ). Inset showing the pole figure of the entire investigated area. **e)** Specimen IC-06. Orientation image of contact between two dissepiments. Points 1 and 2 correspond with selected regions plotted in (III). **f)** Petrographic micrograph of the studied area. Inset showing the pole figure of the entire investigated area. Pole figures were calculated as an orientation distribution function and provided in multiples of uniform distribution intervals of 0.5 for c-axis orientations. Red points correspond to the punctual c-axis orientation of each pixel of selected areas, I (a-b), points 1 and 2 correspond with inner part and lamellar rows of the wall. II (c-d), area 1 marked in the black dotted line. III (d-e) Variation of the points 1 and 2, corresponding with two different rows of fascicle. Coloured circle in the right margin corresponds with the standard colour look-up table (CLUT). Scale bars = 150  $\mu\text{m}$ .



dissepiments, septal stereoplasm and thickenings are lamellar. The septal mesoplasm has been described as granular, granule-fibrous, fibrous and fibro-normal. Semenoff-Tian-Chansky (1974, p. 211-250) stated in the diagnosis of *Axophyllum* that the septal mesoplasm is fibrous, but some of the species described by him (*A. tazoultense*, *A. dibunoides*) show granular mesoplasm and others (*A. pseudokirsopianum*, *A. begaense*) show granule-fibrous mesoplasm. Rodríguez & Somerville (2015) described the septal mesoplasm of *Morenaphyllum* as composed of bundles of microlamellae that comprise pseudofibrous structures. More detailed analyses described above demonstrate that the microstructure of *Morenaphyllum* does not differ greatly from other genera of the subfamily. The piles of lamellae organised in bundles or fascicles occur in the wall and on some lonsdaleoid dissepiments as well as in other genera of the subfamily (*Axophyllum*, *Gangamophyllum*, etc. Rodríguez & Somerville, 2015). On the contrary, the septal microstructure is composed typically of very small fibres (microfibres) oriented upwards in most part of the septa and with low angle in the axial parts. In transverse section, the microfibres of most part of the septa are cut perpendicular to the c-axis, giving a granulate aspect. So, if other Axophyllinae genera show the same structure, the granular microstructure described in some genera and species could be really microfibrillar microstructure as well as in *Morenaphyllum*. The detailed microstructure of other Axophyllinae is being currently studied in order to test this hypothesis.

The septa in *Morenaphyllum* do not show a constant stereoplasm covering the mesoplasm. Thickenings are frequent in many zones of the corallites. They are always lamellar, but do not constitute a complete second phase of secretion of septa. It seems to be identical to most species belonging to the subfamily (Semenoff-Tian-Chansky, 1974; Rodríguez & Somerville, 2015).

*Morenaphyllum* microstructure and crystallographic arrangement show large areas with biogenic properties despite of diagenetic alteration, based on the great

crystallographic control, complex microstructures and crystal morphologies (lamellae) and the robust relation between the structural elements and their microstructure. All this suggest that *Morenaphyllum* skeleton is formed by calcitic hierarchical structures as other Paleozoic corals previously studied by the authors (Coronado *et al.*, 2013, 2015a, 2015b, 2016; Coronado & Rodríguez, 2016).

The great crystallographic control observed in each structural element (septa, stereoplasm, wall, etc.) suggest that epithelial tissue should be almost in contact with biocrystallization area. Some evidences of this hypothesis could be observed in the crystallographic relation of different structural elements. The contact zones of septa and wall and stereoplasm or the dissepiments each other, show a gradual transition between the microstructural elements keeping the crystallographic properties. Some evidences provided above suggest that the fascicles of festoon-like structures could have grown in a competitive growth mode as, for instance the contact between fascicles and their variation of microcrystals size and the abrupt change in crystallographic orientation. Competitive growth mechanisms have been previously identified in Syringoporicae wall (Coronado *et al.*, 2015a).

The morphological and size differences of microstructures, overall in lamellar tissues reveal that the biocrystallization of each zone is should be produce by a specialised tissue of epithelium, as occur with the differences in calcioblastic cell layers in scleractinian (Tambutté *et al.*, 2007; Stolarski *et al.*, 2016). In this particular case, the variations between “scutellate” to “copular” and domical elements with transitions between microlamellae to lamellae suggest that independent of the stages and kinetics of crystallization the precipitation use other elements as substrate of biomineralization.

The wall and stereoplasm have special c-axis distribution as the rotation ca. 40° of some crystal domains (Fig. 5II, Fig. 6II), as occur in some Syringoporicae (Coronado *et al.*, 2015a, 2015b). This feature, always observable in transverse sections, could be inherited of cylindrical

**Figure 6.** CIP analysis of a transverse section of *Morenaphyllum*. F: fibres; L: lamellae;  $\mu$ L: microlamellae; S: septum; St: stereoplasm; W: wall. **a)** Specimen IC-07. Orientation image of a stereoplasm area in contact with a septum. **b)** Petrographic micrograph of studied area showing the lamellar microstructure of stereoplasm and its relation with the fibres of septum. Inset showing the pole figure of the entire investigated area. **c)** Specimen IC-15. Orientation image of the contact between wall area and a septum. Points 1 and 2 correspond with selected regions plotted in (II). **d)** Petrographic micrograph of the studied area showing the relations between two microstructures. Inset showing the pole figure of the entire investigated area. **e)** Specimen IC-18. Orientation image of the stereoplasm area in contact with septa. Points 1 and 2 correspond with selected regions plotted in (III). **f)** Petrographic micrograph of the studied area. Inset showing the pole figure of the entire investigated area. Pole figures were calculated as an orientation distribution function and provided in multiples of uniform distribution intervals of 0.5 for c-axis orientations. Red points correspond to the punctual c-axis orientation of each pixel of selected areas. I (**a-b**) C-axis orientation of the point 1, corresponding with the blocky cement of coral calyx. II (**c-d**) Variation of the points 1 and 2, corresponding with the insertion zone of septum in the wall and the fibres of septum. III (**d-e**) Variation of the points 1 and 2, corresponding with microlamellae and lamellae of stereoplasm. Coloured circle in the right margin corresponds with the standard colour look-up table (CLUT). Note that the CLUT has been rotated to adapt to the micrographs selected and the figure composition in **d)** and **e)**. Scale bars = 150  $\mu$ m.

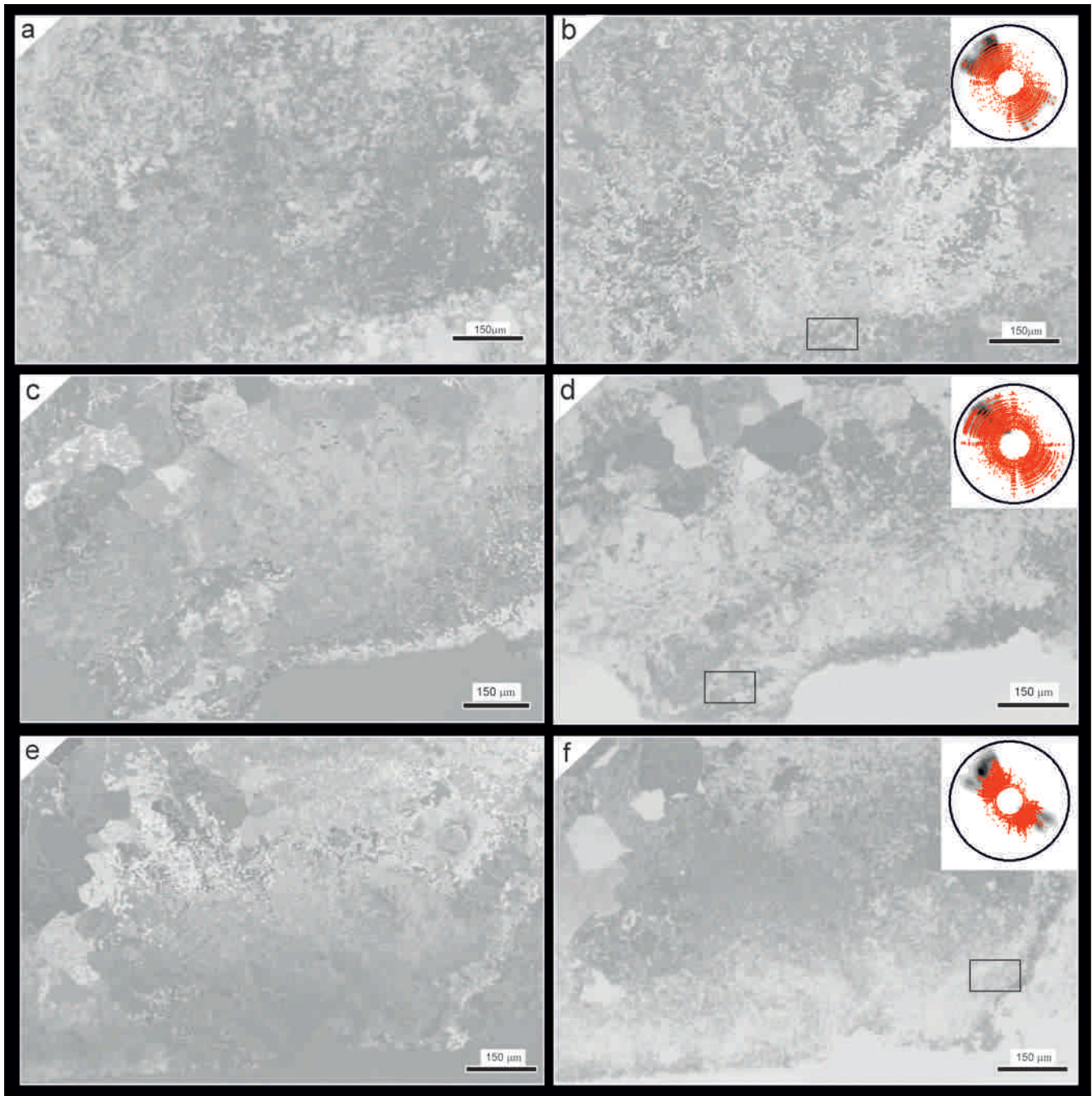


**Figure 7.** Misorientation image in grey scale colour, showing the variations of colouration due to diagenetical alteration. **a-b)** Specimen IC-14. **c-d)** Specimen IC-07. **e-f)** Specimen IC-01. **a, c, e)** North-south misorientation image. **b, d, f)** Inclination variation misorientation image. Note that strong changes in coloration indicate strong changes in misorientation. Insets represent the pole figures of altered areas (square) in each COI studied. Red points correspond to the punctual c-axis orientation of each pixel of selected areas. Scale bars = 150 µm.

nature of Paleozoic corals in origin represented by their close relatives as Tabulaconids and Cotonids, which had a cylindrical to conical structuration of skeleton (Scrutton, 1997). Other Rugosa studied as *Calceola sandalina* have some inherited features as turbostratic distribution in some crystallographic planes, which occur in some specific areas due to its complex inner structuration. This

indicate that Rugosa, due to its supra-specialization and the formation of complex structural elements (as special septa, dissepimentarium, axial structures), could have modified the mechanisms of building skeleton at meso- and microscale, but as *Calceola* (Coronado *et al.*, 2016) and *Morenaphyllum* skeleton reveal the basal building mechanisms are kept along time.

Other remarkable similarities with *Calceola* have been observed: the composed septa described by Coronado *et al.* (2016) have narrow azimuthal distribution similar to *Morenaphyllum*, in spite of different microstructure, lamellar in *Calceola* and fibrous in *Morenaphyllum*, indicating that mechanism of biocrystallization of septa are quite similar, differentiated by the morphology and microstructure of septa. Other similar characteristic observed in *Morenaphyllum* is the formation of fibrous domains in the external fringes of dissepiments, and wall with fasciculate and tepee-like structures. These points probably could equivalent to desmocites scars observed in *Calceola*. The fibres in these external parts could favour the anchorage of epithelial tissue of polyp to skeleton.

These characteristics shed light about the unknown biocrystallization processes of Paleozoic corals. The similarities and differences between this clade suggest that should be studied in depth comparing to the superfamily level, even orders. Although this study is a starting point about the knowledge of the Axophyllinae and their microstructural variations and their possible origin in the evolution of Rugosa it should be analysed.

## 6. CONCLUSIONS

The in deep study about the microstructure and crystallography of *Morenaphyllum* highlights:

- 1) The crystallographic orientation study reveals that the skeletons studied still partially preserve their biogenic features.
- 2) Thick wall and stereoplasm are mainly composed of lamellae, with some domains of fibres in the inner fringe.
- 3) The septa are formed by sort irregular fibres that in section give the appearance of pseudograins.
- 4) There is a gradual transition between the different microstructural domains, characteristic of all Paleozoic corals, when the biogenic properties are preserved. The crystallographic orientation between the microstructures is coherent and kept along domains and structural elements.
- 5) The microstructure of *Morenaphyllum* is coherent with that described previously in other Axophyllinae.
- 6) The microstructural features suggest that the studied skeletons are composed of hierarchical structures, similarly to other Paleozoic corals.
- 7) The crystallographical properties suggest a common evolutionary pathway between Cambrian coralomorphs and Rugosa, which should be studied to understand the evolutionary biomineralization processes.

## ACKNOWLEDGEMENTS

The present research has been carried out with the funds provided by the Research Projects CGL-30922BTE and CGL2016-78738-P of the Ministerio de Economía y Competitividad. Ismael Coronado acknowledges financial support through a Research Grant supported by the Sociedad Española de Paleontología, which has enabled to improve the CIP system. The ultrathin sections used for this study have been prepared by Isabel Díaz Mejías. We thank the reviewers (Esperanza Fernández-Martínez and Olga Kossovaya) and the editor (Gonzalo Jiménez Moreno) for their help and constructive comments on the text.

## REFERENCES

- Abràmoff, M.D., Magalhães, P.J. & Ram, S.J. 2004. Image processing with ImageJ. *Biophotonics International*, 11, 36-42.
- Barret, S. 1997. Image analysis and the internet. *Scientific Data Management*, 1, 18-25.
- Chacón, J., Delgado-Quesada, M.Y. & Garrote, A. 1974. Sobre la existencia de dos diferentes dominios de metamorfismo regional en la banda Elvas-Badajoz-Córdoba (Macizo Hespérico Meridional). *Boletín Geológico y Minero*, 85, 713-717.
- Colmenero, J.R., Fernandez, L.P., Moreno, C., Bahamonde, J.R., Barba, P., Heredia, N. & Gonzalez, F. 2002. Carboniferous. In: *The Geology of Spain* (eds. Gibbons, W. & Moreno, T.). Geological Society, Bath, United Kingdom, 93-116.
- Coronado, I. & Rodríguez, S. 2016. Biomineral structure and crystallographic arrangement of cerioid and phaceloid growth in corals belonging to the Syringoporicae (Tabulata, Devonian–Carboniferous): a genetic reflection. *Geological Magazine*, 153, 718-742; doi: 10.1017/S0016756815000862.
- Coronado, I., Pérez-Huerta, A. & Rodríguez, S. 2013. Primary biogenic skeletal structures in *Multiithecopora* (Tabulata, Pennsylvanian). *Palaeogeography, Palaeoclimatology, Palaeoecology*, 386, 286-99; doi: 10.1016/j.palaeo.2013.05.030.
- Coronado, I., Pérez-Huerta, A. & Rodríguez, S. 2015a. Computer-integrated polarisation (CIP) in the analysis of fossils: a case of study in a Palaeozoic coral (*Sinopora*, Syringoporicae, Carboniferous). *Historical Biology*, 27, 1098-1112; doi: 10.1080/08912963.2014.938236.
- Coronado, I., Pérez-Huerta, A. & Rodríguez, S. 2015b. Crystallographic orientations of structural elements in skeletons of Syringoporicae (tabulate corals, Carboniferous): implications for biomineralization processes in Palaeozoic corals. *Palaeontology*, 58, 111-132; doi: 10.1111/pala.12127.
- Coronado, I., Fernández-Martínez, E., Rodríguez, S. & Tourneur, F. 2015c. Reconstructing a Carboniferous

- inferred coral-alcyonarian association using a biomineralogical approach. *Geobiology*, 13, 340-356; doi: 10.1111/gbi.12133.
- Coronado, I., Pérez-Huerta, A. & Rodríguez, S. 2016. Analogous biomineralization processes between the fossil coral *Calceola sandalina* (Rugosa, Devonian) and other Recent and fossil cnidarians. *Journal of Structural Biology*, 196, 173-186; doi: 10.1016/j.jsb.2016.06.013.
- Cózar, P. & Rodríguez, S. 1999. Propuesta de nueva nomenclatura para las unidades del Carbonífero Inferior del sector Norte del Área del Guadiato (Córdoba). *Boletín Geológico y Minero*, 110, 237-254.
- Cózar, P. & Rodríguez, S. 2000. Caracterización estratigráfica y sedimentológica del Visense superior de Sierra Boyera (Área del Guadiato, SO de España). *Revista de la Sociedad Geológica de España*, 13, 91-103.
- Cummins, R.C., Finnegan, S., Fike, D.A., Eiler, J.M. & Fischer, W.W. 2014. Carbonate clumped isotope constraints on Silurian ocean temperature and seawater  $\delta^{18}\text{O}$ . *Geochimica et Cosmochimica Acta*, 140, 241-258; doi: 10.1016/j.gca.2014.05.024.
- Dalbeck, P., England, J., Cusack, M. & Fallick, A.E. 2006. Crystallography and chemistry of the calcium carbonate polymorph switch in *M. edulis* shells. *European Journal of Mineralogy*, 18, 601-609; doi: 10.1127/0935-1221/2006/0018-0601.
- Delgado-Quesada, M., Liñán, E., Pascual, E. & Pérez-Lorente, F. 1977. Criterios para la diferenciación de dominios en Sierra Morena central. *Studia Geologica*, 12, 75-90.
- Falces, S. 1997. Borings, embeddings and pathologies against microstructure. New evidences on the nature of the microstructural elements in rugose corals. *Boletín de la Real Sociedad Española de Historia Natural*, 92, 99-116.
- Gómez-Herguedas, A. & Rodríguez, S. 2005. Estudio de los corales rugosos con disepimientos del Serpujoviense (Mississippiense) de la sección de La Cornuda (Córdoba, España). *Coloquios de Paleontología*, 55, 51-101.
- Gorsky, I.I. 1938. Kamennougolnie korally Novoi Zemli. *Trudy Nauchno-Issledovatel'skogo Instituta Geologii Arktiki*, 93, 1-221.
- Gorsky, I.I. 1951. Kamennougolnye i permskie korally Novoj Zemli. *Trudy Nauchno-Issledovatel'skogo instityite geologii Arktiki*, 32, 1-168.
- Grellet-Tinner, G., Sim, C.M., Kim, D.H., Trimby, P., Higa, A., An, S.L., Oh, H.S., Kim, T.J. & Kardjilov, N. 2011. Description of the first lithostrotian titanosaur embryo in ovo with Neutron characterization and implications for lithostrotian Aptian migration and dispersion. *Gondwana Research*, 20, 621-629; doi: 10.1016/j.gr.2011.02.007.
- Heilbronner, R. 2000. Automatic grain boundary detection and grain size analysis using polarization micrographs or orientation images. *Journal of Structural Geology*, 22, 969-981; doi: 10.1016/S0191-8141(00)00014-6.
- Heilbronner, R. & Barret, S. (eds.). 2014. *Image Analysis in Earth Sciences - Microstructures and Textures of Earth Materials*. Springer, London, 520 pp.
- Heilbronner, R.P. & Pauli, C. 1993. Integrated spatial and orientation analysis of quartz c-axes by computer-aided microscopy. *Journal of Structural Geology*, 15, 369-382; doi: 10.1016/0191-8141(93)90133-U.
- Kato, M. 1963. Fine skeletal structures in Rugosa. *Journal of the Faculty of Science, Hokkaido University. Serie. 4*, 571-630.
- Lafuste, J. 1970. Lames ultra-minces a faces polies. Procède et application a la microstructure des Madreporaires fossiles. *Comptes rendus de l'Académie des Sciences, Paris*, 270, 679-81.
- Lafuste, J. 1978. Modalités de passage des lamelles aux fibres dans la muraille de Tabules (Michelinidae) du Devonien et du Permien. *Geobios*, 11, 405-08.
- Lafuste, J. 1981. Structure et microstructure de *Dendropora Michelin* 1846 (Tabulata, Devonien). *Bulletin de la Société Géologique de France*, 23, 271-77; doi: https://doi.org/10.2113/gssgfbull.S7-XXIII.3.271.
- Lafuste, J. 1983. Passage des microlamelles aux fibres dans le squelette d'un Tabulé "michelini-morphe" du Viséen du Sahara algérien. *Geobios*, 16, 755-61; doi: https://doi.org/10.1016/S0016-6995(83)80092-8.
- Lafuste, J. & Plusquellec, Y. 1985. Attribution de "*Michelinia*" compressa Michelin, 1847 au genre *Yavorskia* Fomitchev (Tabule, Tournaisien). *Geobios*, 18, 381-387.
- Oekentorp, K. 1984. Aragonite and diagenesis in Permian corals. *Palaeontographica Americana*, 54, 282-292.
- Oekentorp, K. 2001. Review on diagenetic microstructures in fossil corals - a controversial discussion. *Bulletin of Tohoku University Museum*, 1, 193-209.
- Pérez-Huerta, A., Cusack, M. & England, J. 2007. Crystallography and diagenesis in fossil Craniid brachiopods. *Palaeontology*, 50, 757-763; doi: 10.1111/j.1475-4983.2007.00688.x.
- Pérez-Lorente, F. 1979. *Geología de la zona Ossa-Morena al norte de Córdoba (Pozoblanco-Belmez-Villaviciosa de Cordoba)*. Tesis Doctoral Universidad de Granada, 281, 1-340.
- Poty, E. 1981. Recherches sur les Tétracoralliaires et les Hétérocóraliaires du Viséen de la Belgique. *Mededelingen Rijks Geologische Dienst*, 35, 1-161.
- Rodríguez, S. 1984. *Corales Rugosos del Este de Asturias*. Ed. Complutense 109/84, 1-529.
- Rodríguez, S. 1989. Lamellar microstructure in Palaeozoic corals: origin and use in taxonomy. *Memoires of the Association of Australasian Palaeontologists*, 8, 157-68.
- Rodríguez, S. 2004. Taphonomic alterations in upper Viséan dissepimented rugose corals from the Sierra del Castillo unit (Carboniferous, Córdoba, Spain). *Palaeogeography, Palaeoclimatology, Palaeoecology*, 214, 135-153; doi: /10.1016/j.palaeo.2004.07.026.
- Rodríguez, S. & Rodríguez-Curt, L. 2002. Reconstrucción de una plataforma carbonatada Visense no preservada en el área del Guadiato (Córdoba, SO de España). *Geogaceta*, 32, 283-286.
- Rodríguez, S. & Said, I. 2010. Descripción de los corales rugosos del Visense superior de Peñarroya-Pueblonuevo (Córdoba) y El Casar (Badajoz). *Coloquios de Paleontología*, 58, 7-28.
- Rodríguez, S. & Somerville, I.D. 2015. The Axophyllinae from SW Spain: a review. *Boletín de la Real Sociedad Española de Historia Natural*, 108, 81-138.
- Rodríguez, S., Somerville, I.D., Cózar, P., Coronado, I. & Said, I. 2016. Inventory and analysis of the distribution

- of Viséan corals from the Guadiato Area (Córdoba, SW Spain). *Spanish Journal of Palaeontology*, 31, 181-220.
- Sayutina, T.A. 1973. Niznekamennougolnie koralli severnogo Urala. Podotriad Acrophyllina. *Trudy Paleontologicheskogo Instituta*, 140, 1-168.
- Scrutton, C.T. 1997. The Palaeozoic corals, I: origins and relationships. *Proceedings of the Yorkshire Geological and Polytechnic Society*, 51, 177-208; doi: 10.1144/pygs.51.3.177.
- Semenoff-Tian-Chansky, P. 1974. Recherches sur les Tétracoralliaires du Carbonifère du Sahara Occidental. *Editions du Centre Nationale de la Recherche Scientifique, Ser. 6, Science de la Terre*, 30, 1-316.
- Sorauf, J.E. 1971. Microstructure in the exoskeleton of some Rugosa (Coelenterata). *Journal of Paleontology*, 45, 23-31.
- Sorauf, J.E. 1978. Original structure and composition of Permian rugose and Triassic scleractinian corals. *Palaeontology*, 21, 321-339.
- Sorauf, J.E. 1983. Primary biogenic structures and diagenetic history of *Timorphyllum wanneri* (Rugosa), Permian, Timor, Indonesia. *Memoirs of the Association of Australasian Palaeontologists*, 1, 275-288.
- Stolarski, J., Bosellini, F.R., Wallace, C.C., Gothmann, A.M., Mazur, M., Domart-Coulon, I., Gutner-Hoch, E., Neuser, R.D., Levy, O., Shemesh, A. & Meibom, A. 2016. A unique coral biomineralization pattern has resisted 40 million years of major ocean chemistry change. *Scientific Reports*, 6, 27579; doi: 10.1038/srep27579.
- Tambutté, E., Allemand, D., Zoccola, D., Meibom, A., Lotto, S., Caminiti, N. & Tambutté, S. 2007. Observations of the tissue-skeleton interface in the scleractinian coral *Stylophora pistillata*. *Coral Reefs*, 26, 517-529; doi: 10.1007/s00338-007-0263-5.
- Vischer, N.O.E., Huls, P.G. & Woldringh, C.L. 1994. Object-Image: an interactive image analysis program using structured point collection. *Binary*, 6, 160-166.

